ELECTROMAGNETIC CHARACTERISTICS COMPARISONOF PERMANENT MAGNET ASSISTED SYNCHRONOUS RELUCTANCE MOTOR AND SYNCHRONOUS RELUCTANCE MOTOR

Hien Nguyen Thi Minh[1,*], Quang Anh Nguyen[4], Chuong Trinh Trong[1], Cuong Nguyen Tien[2], Huy Pham Canh[3], Viet Nguyen Nga[4], Vuong Dang Quoc[4]

DOI: https://doi.org/10.57001/huih5804.2026.106

ABSTRACT

As global energy-saving demands rise, synchronous reluctance motors (SynRM) have emerged as a promising alternative to conventional permanent-magnet synchronous motors, helping to mitigate the supply chain risks associated with rare-earth materials. However, pure SynRMs are hindered by inherent drawbacks, including low power factors, relatively low torque density, and high torque ripples. To overcome these limitations, permanent magnets can be inserted into the rotor's flux barriers to create a permanent-magnet-assisted synchronous reluctance motor (Pma-SynRM). This paper details the design of a 0.75kW Pma-SynRM and comprehensively compares its characteristics such as torque, flux linkage, inductance, and power factor with a pure SynRM of the same power rating using finite element analysis (FEA). The simulation results demonstrate that the Pma-SynRM topology effectively addresses the disadvantages of the conventional SynRM, achieving a 28% increase in electromagnetic torque and a 24% improvement in the power factor. These findings confirm that the Pma-SynRM is an efficient, high-performance, and cost-effective alternative for modern industrial applications.

Keywords: *Synchronous reluctance motor, permanent-magnet-assisted synchronous reluctance motor, finite element method.*

[1]School of Electrical and Electronic Engineering, Hanoi University of Industry, Vietnam

[2]School of Mechanical Engineering, Hanoi University of Science and Technology, Vietnam

[3]School of Economy, Hanoi University of Science and Technology, Vietnam

[4]School of Electrical and Electronic Engineering, Hanoi University of Science and Technology, Vietnam

[*]Email: hienntm@haui.edu.vn

Received: 19/3/2026

Revised: 15/4/2026

Accepted: 29/5/2026

1. INTRODUCTION

Induction motors have long dominated the industrial manufacturing sector, primarily due to their robust reliability, high overload capacity, and cost-effective production [[1, 2]. While these conventional machines generally meet the IE3 efficiency standards established by IEC 60034-1, upgrading them to the more stringent IE4 level presents significant technical challenges [3, 4]. Simultaneously, escalating global imperatives for energy conservation and the reduction of CO emissions largely driven by European regulatory policies are accelerating the transition from traditional motors to advanced machines offering superior efficiency, precise controllability, and enhanced fault tolerance [5, 6]. In this landscape, the synchronous reluctance motor (SynRM) has emerged as a highly promising alternative to the standard induction motor. However, widespread industrial adoption of pure SynRMs has been hindered by inherent performance limitations, most notably a low power factor, significant torque ripple, and relatively low torque density compared to its power rating [7].

To mitigate these drawbacks, an effective solution involves integrating permanent magnets (PMs) into the rotor's flux barriers. Although the resulting architecture resembles an interior PM synchronous motor (IPMSM), it utilizes a substantially smaller volume of magnetic material. Consequently, it exhibits a lower permanent magnet flux linkage and relies primarily on reluctance torque for its mechanical output. This optimized configuration is widely recognized as the permanent magnet-assisted synchronous reluctance motor (PMa-SynRM).

A primary challenge in the SynRM design is the complex rotor geometry. While the stator is identical to that of an induction motor of the same rating, the rotor contains neither squirrel-cage bars nor field windings. Instead, multiple flux barriers are strategically engineered to maximize the inductance saliency ratio (L_d/L_q). Literature indicates two common geometric configurations for these barriers:

- Segmented flux barriers: These are designed using geometric parameters aligned to achieve an optimal saliency ratio. This type is prevalent in modern manufacturing due to its simpler punching die, high mechanical strength, and the feasibility of inserting permanent magnets into the rotor air gaps.

- Concentrated flux barriers: Constructed based on flux lines parallel to the magnetic flux paths, this configuration yields a very high saliency ratio. However, due to its geometric complexity, it is reserved for applications requiring exceptionally high torque and power density.

To enhance both torque and power factor, permanent magnets are inserted to transform the machine into a PMa-SynRM. Designing high-performance SynRMs requires a synergy of classical analytical methods and modern finite element analysis (FEA) tools; however, a comprehensive, step-by-step design procedure remains scarce in existing literature. In Vietnam, industrial applications remain dominated by induction motors. As the nation's industrialization and modernization progress, sophisticated production lines demand drive motors with higher efficiency, improved controllability, and superior fault tolerance. These motors must also deliver a high torque density and a power factor that satisfies national grid requirements. While the PMa-SynRM meets these criteria, domestic publications regarding its detailed design methodology and comparative evaluations against pure SynRMs are limited.

This paper details the design of a SynRM based on reference parameters given by the ABB company, followed by the integration of permanent magnets into the flux barriers to quantify performance enhancements. A comprehensive comparison of torque, flux linkage, inductance, and power factor between the two topologies is presented.

2. THEORETICAL BACKGROUND

The phasor diagrams in the *d-q* reference frame of a SynRM and PMa-SynRM are shown in Figure 1.

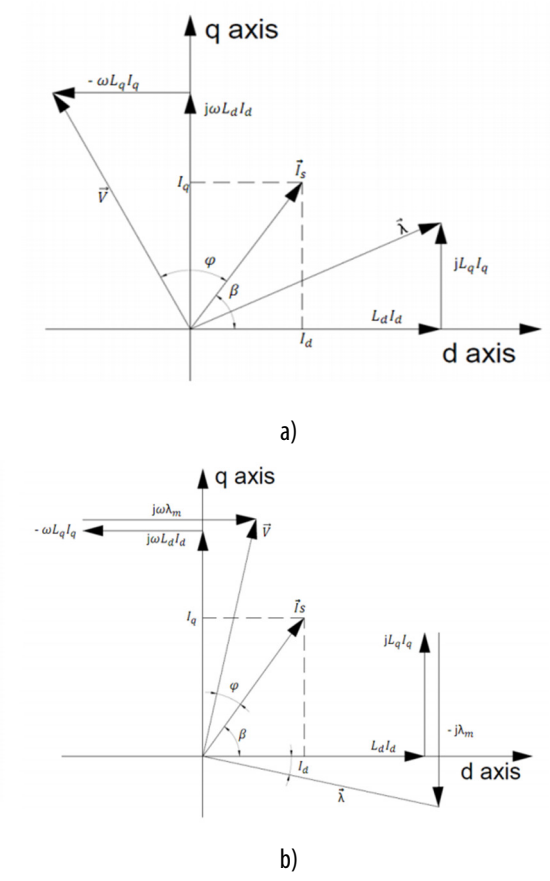

Figure 1. Phasor diagram for [8]: (a) SynRM; (b) PMa-SynRM

Based on the PMa-SynRM presented in [8, 9], the voltage equations of the SynRM in the d-q axis can be expressed as follows:

$$V_d = R_s i_d + \frac{d\lambda_d}{dt} - \omega\lambda_q = R_s i_d + \frac{d\lambda_d}{dt} - \omega L_q i_q \quad (1)$$

$$V_q = R_s i_q + \frac{d\lambda_q}{dt} + \omega\lambda_d = R_s i_q + \frac{d\lambda_q}{dt} + \omega L_d i_d \quad (2)$$

The voltage equations can be rewritten by using the relationship between inductance and flux linkage, in d-q reference frame, they are expressed as [9]:

$$\lambda_d = \lambda_d(i_d, i_q) = L_d(i_d, i_q) i_d, \quad (3)$$

$$\lambda_q = \lambda_q(i_d, i_q) = L_q(i_d, i_q) i_q, \quad (4)$$

so that V_d and V_q can be calculated as [9]:

$$V_d = R_s i_d + L_d \frac{di_d}{dt} - \omega L_q i_q, \quad (5)$$

$$V_q = R_s i_q + L_q \frac{di_q}{dt} + \omega L_d i_d. \quad (6)$$

In the PMa-SynRM, the PMs are placed in the direction of the q-axis flux. The d-axis flux linkage equation remains the same, but the q-axis becomes [9, 10]:

$$\lambda_q = \lambda_q(i_d, i_q) = L_q(i_d, i_q) i_q - \lambda_m \quad (7)$$

The voltage equations of the PMa-SynRM in the d-q axis can be expressed as follows [9]:

$$V_d = R_s i_d + L_d \frac{di_d}{dt} - \omega L_q i_q + \lambda_m \omega, \quad (8)$$

$$V_q = R_s i_q + L_q \frac{di_q}{dt} + \omega L_d i_d, \quad (9)$$

where λ_m is the PM flux linkage; V_d and V_q are the stator voltage in the d- and q-axis respectively; λ_d and λ_q are the flux linkage in the d- and q-axis respectively; i_d and i_q are the current in the d-and q-axis respectively; R_s is stator resistance; ω is the rotor electrical angular velocity; L_d and L_q are the inductances in d- and q-axis respectively.

The power factor is given by [11]:

$$IPF = \cos(\varphi) = cos\left(tan^{-1}\left(\frac{\frac{L_d i_d}{L_q i_q} + \frac{i_q}{i_d}}{\frac{L_d}{L_q} - 1}\right)\right) = \frac{(\xi - 1)}{\sqrt{\xi^2 \frac{1}{sin^2\beta} + \frac{1}{cos^2\beta}}}$$

$$= (\xi - 1)\sqrt{\frac{sin(2\beta)}{2(tan\,\beta + \xi^2\, cot\,\beta)}},$$

$$\text{for the saliency ratio, } \xi = \frac{L_d(i_d)}{L_q} \quad (10)$$

where φ is the phase angle and β is the current angle.

The internal power factor is highly dependent of the machine saliency ratio and is maximized when the $\tan(\beta) = \sqrt{\xi}$, one has [11]:

$$IPF|_{max} = \cos(\varphi)\,|_{max} = \frac{\xi - 1}{\xi + 1} \quad (11)$$

The electromagnetic torque is then produced by the product of flux linkage and the current that flows through the coil, the torque for the SynRM is as follows [9]:

$$T_e = \frac{3n_p}{2}\left(L_d - L_q\right) i_d i_q = \frac{3n_p}{2}\left(L_d - L_q\right) I_{mag}^2 \frac{\sin(2\beta)}{2} \quad (12)$$

where I_{mag} is the magnitude of the current and n_p is the number of pole pairs in machine.

For a PMa-SynRM, the electromagnetic torque then becomes [9]:

$$T_e = \frac{3n_p}{2}\left(\lambda_m i_d + \left(L_d - L_q\right) i_d i_q\right), \quad (13)$$

or if written with current magnitude and current angle

$$T_e = \frac{3n_p}{2}\left(\lambda_m I_{mag} \cos\beta + (L_d - L_q) I_{mag}^2 \frac{\sin(2\beta)}{2}\right) \quad (14)$$

3. SIMULATION RESULTS

Based on the theoretical formulations presented in Section 2, both the synchronous reluctance motor (SynRM) and the permanent magnet-assisted synchronous reluctance motor (PMa-SynRM) were designed and analyzed using finite element analysis (FEA). To ensure a fair comparison, both machines share identical stator geometry and operating conditions, while the rotor of the PMa-SynRM is modified by embedding NdFeB permanent magnets within the flux barriers. The design parameters of the SynRM are given in Table 1, Table 2 and Table 3. It can be seen that Tables 2 ÷ 4 summarize the key design parameters of the stator, rotor, and permanent magnets for both machines. The stator adopts a conventional 36-slot structure with appropriate dimensions (76mm inner diameter and 125mm outer diameter), ensuring adequate magnetic loading and thermal performance for a 0.75kW rating. The relatively high number of turns per coil enhances magnetomotive force, contributing to torque production. The rotor design employs three flux barriers per pole, which is an effective compromise between achieving a high saliency ratio (L_d/L_q) and maintaining mechanical robustness. The selected rotor dimensions also ensure a small air gap, improving electromagnetic coupling. For the PMa-SynRM, the NdFeB magnets with high residual flux density (1.21T) are strategically embedded within the flux barriers. The graded magnet dimensions across layers optimize flux distribution while minimizing material usage. Overall, these design choices enable enhanced torque capability and improved power factor while preserving structural integrity and cost efficiency.

Table 1. Initial parameters of the SynRM

Parameter	Value	Unit
Power	0.75	kW
Speed	1500	rpm
Pole number	4	pole
Terminal voltage	400	V
Efficiency	82.5	%
Power factor	0.72	

Table 2. Stator calculation results

Parameter	Value	Unit
Inner diameter	76	mm
Outer diameter	125	mm
Motor length	70	mm
Number of slots	36	slot
Number of turns per coil per phase	85	turn

Table 3. Optimized rotor dimensions

Parameter	Value	Unit
Outer diameter	75.5	mm
Shaft diameter	24	mm
Number of flux barriers	3	

The PM dimensions for the PMa-SynRM are given in Table 4.

Table 4. PM dimensions

Parameter	Value	Unit
PM type	NdFeB	
Residual magnetic density	1.21	T
Magnetic resistance	-995	H
Length magnet 1	20.9	mm
Width magnet 1	4.7	mm
Length magnet 2	13.6	mm
Width magnet 2	3.8	mm
Length magnet 3	8.8	mm
Width magnet 3	3.3	mm

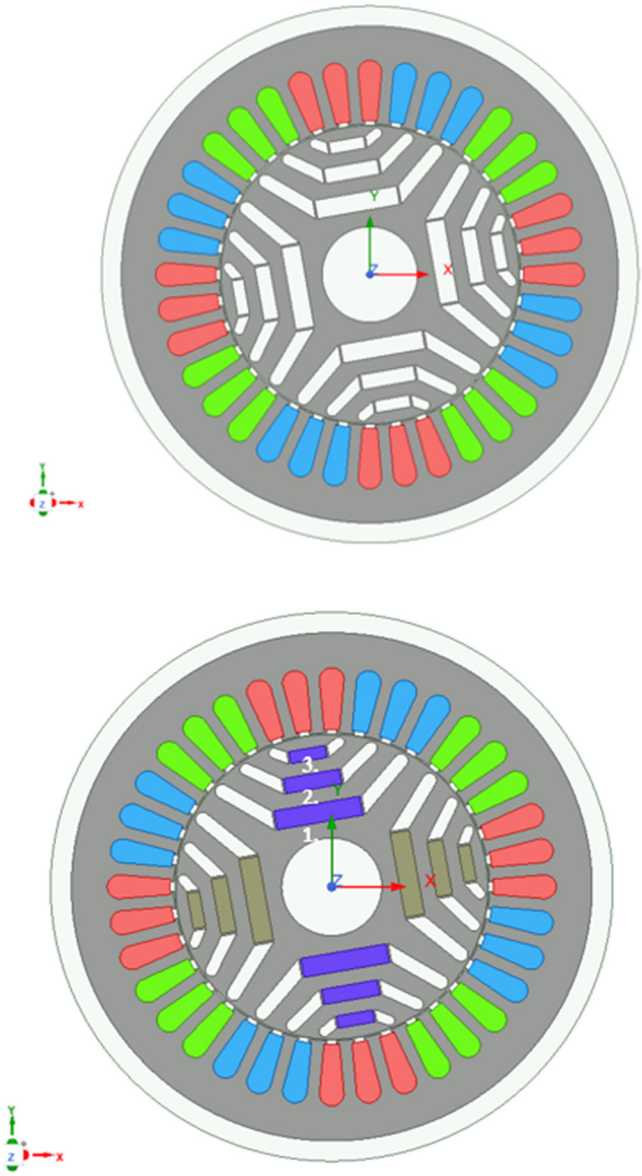

Figure 2. 2D model of SynRM (left) and of Pma-SynRM (right)

The 2D model of SynRM and PMa-SynRM is presented in Figure 2. The SynRM (left) has a 4-pole rotor with three flux barriers per pole, creating high saliency for reluctance torque. The Pma-SynRM (right) uses the same three flux barrier structure per pole, with permanent magnets inserted into the designed air gaps.

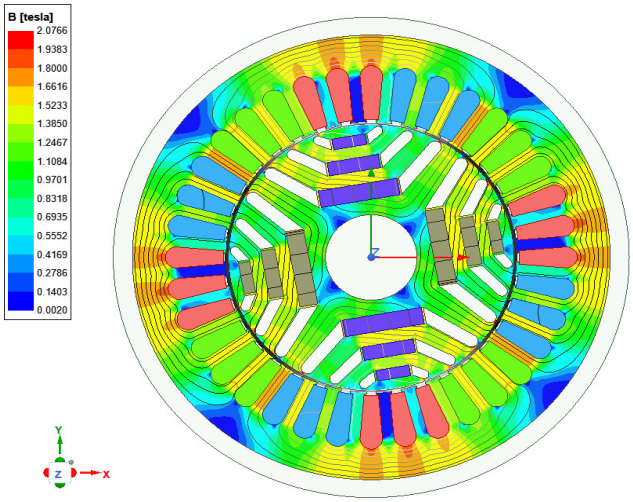

(a)

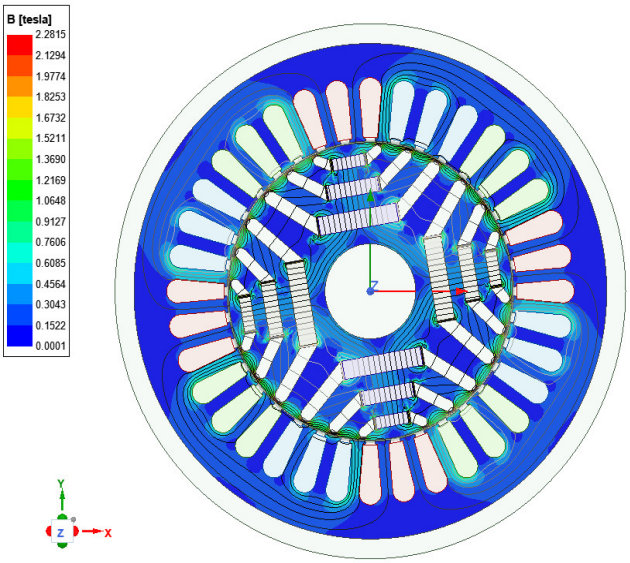

(b)

Figure 3. PMa-SynRM d--axis (a) and q-axis(b) magnetic flux densities

The distribution of magnetic flux in the d- and q-axis for both motors is presented in Figure 3 and Figure 4. It can be seen that under the maximum d-axis current (a) (current angle = 0 degrees), the influence of the permanent magnets causes the flux density in the flux-carrying iron portions of the PMa-SynRM rotor core to reach 1.63T, which is higher than the 1.52T observed in

the pure SynRM under identical conditions. Consequently, careful design consideration must be given to the magnet strength and the thickness of both the iron ribs and tangential bridges to prevent deep core saturation. Furthermore, at maximum q-axis (b) current (current angle = 90 degrees), the flux density distribution indicates that modifying the regions between the air flux barriers and the rotor iron segments to reduce L_d (such as by increasing the air-gap length) requires a careful trade-off between controlling air-gap flux density and maintaining the rotor's mechanical integrity.

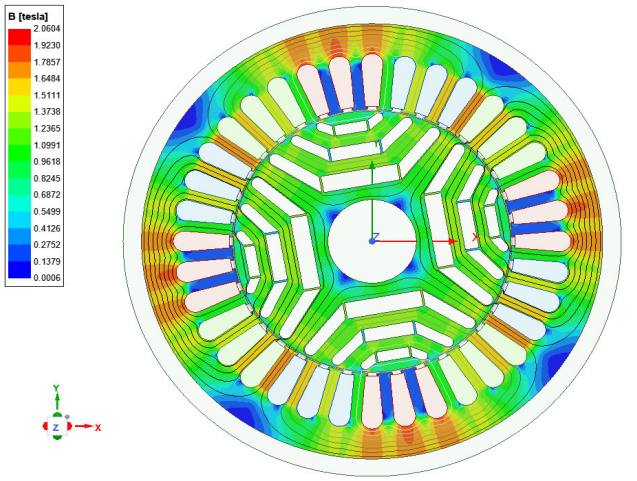

(a)

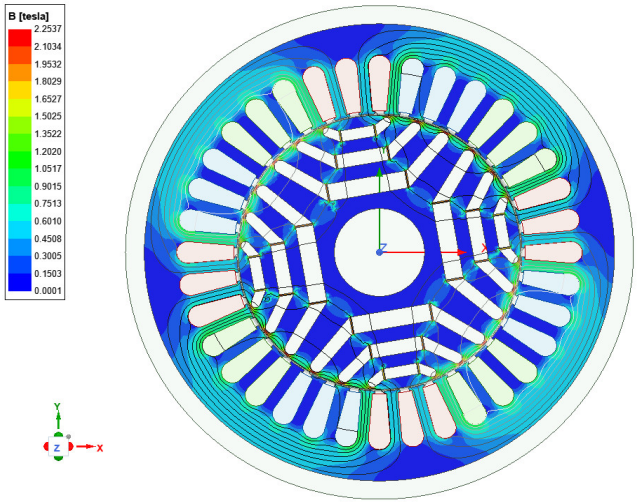

(b)

Figure 4. SynRM d-axis (a) and q-axis(b)magnetic flux densities

The static torque characteristics of both motors is given in Figure 5. It can be seen that the static torque of the PMa-SynRM reaches 5.75Nm, which is 22.7% higher than that of a conventional SynRM of the same power rating, primarily due to the addition of permanent magnet torque. However, the reluctance torque component remains dominant and significantly higher, which is the key distinguishing feature between the PMa-SynRM and IPMSM.

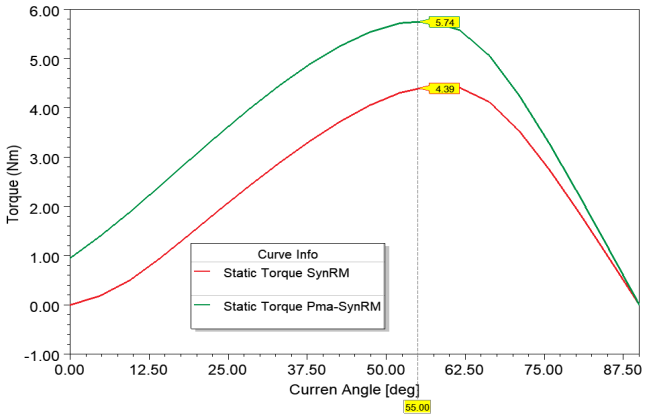

Figure 5. Static torque of SynRM and Pma-SynRM

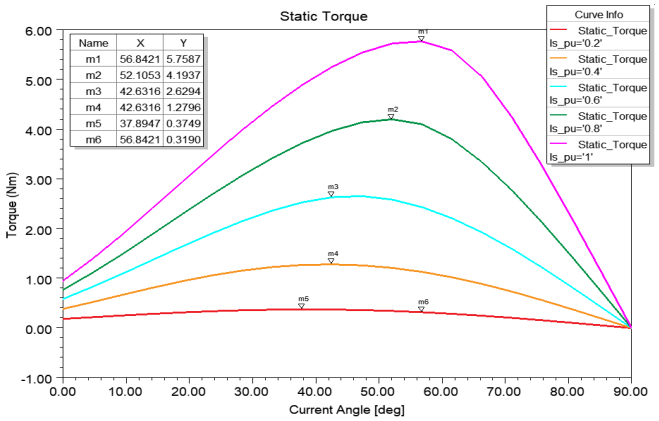

Figure 6. Static torque characteristics versus stator current variation of PMa-SynRM

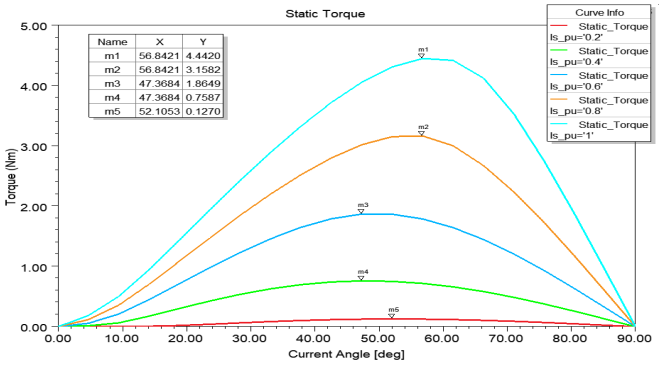

Figure 7. Static torque characteristics versus stator current angle variation of SynRM

In Figures 6 and 7, when analyzing the static torque characteristics under varying stator currents and current angles, the PMa-SynRM consistently produces higher torque than the pure SynRM at identical current levels. Overall, as shown in Figure 8, the nominal electromagnetic torque improves from 4.2Nm in the SynRM to 5.4Nm in the PMa-SynRM, representing a significant 28% increase.

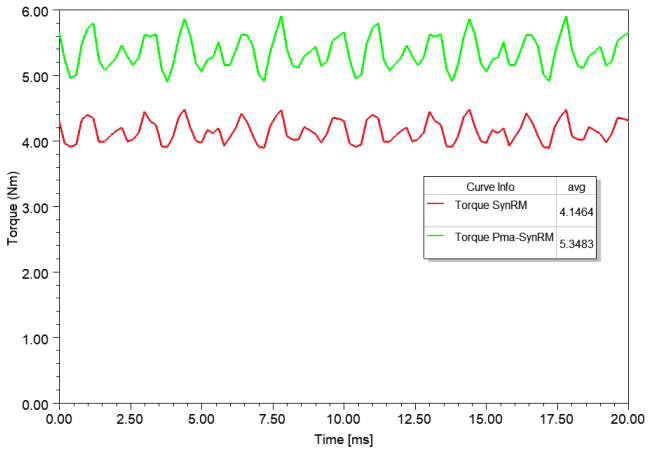

Figure 8. Comparison of electromagnetic torque between the two motors

The flux-linkage and saliency ratio is pointed out in Figure 9 and Figure 10.

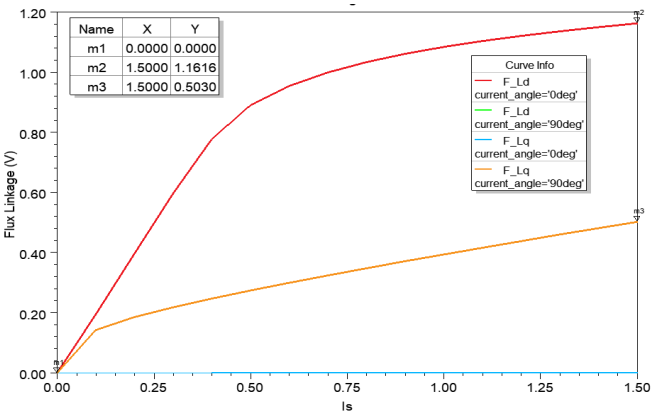

Figure 9. Flux-linkage characteristics of SynRM

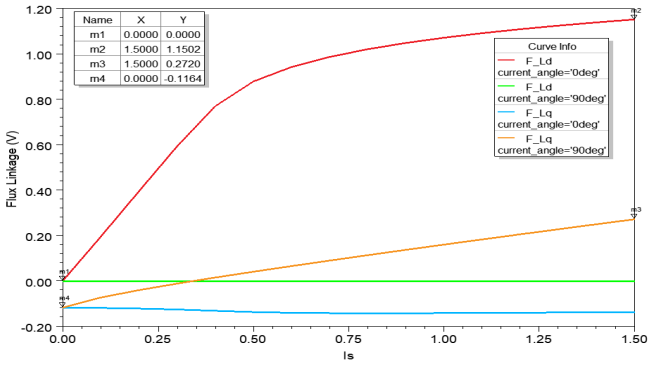

Figure 10. Flux-linkage characteristics of PMa-SynRM.

Figure 9 illustrates the flux-linkage characteristics of the pure SynRM. The difference between the d-axis and q-axis flux-linkage curves forms a closed area (locus). The d-axis characteristic is strongly influenced by the saturation behavior of the core material, whereas the q-axis curve is nearly linear because its magnetic path predominantly passes through the air barriers and air gap. A larger enclosed area corresponds to a higher ratio of d-axis to q-axis flux linkage, which directly increases the inductance saliency ratio (L_d/L_q) and enhances the reluctance torque. In Figure 10, the PMa-SynRM flux-linkage characteristics show a significantly larger enclosed locus area compared to the pure SynRM. Additionally, the permanent magnets contribute a distinct flux-linkage component of -0.1164Wb, further augmenting the total torque.

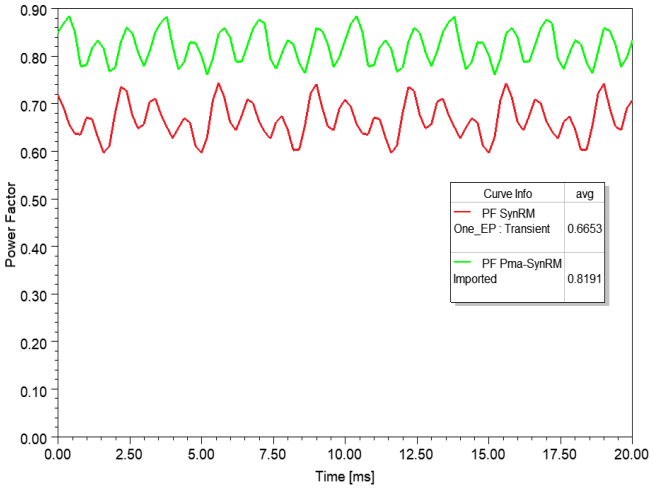

Figure 11. Comparison of power factor between two motors

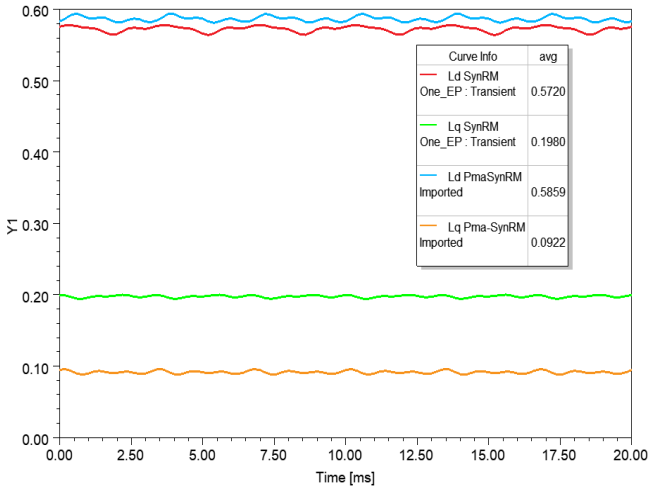

Figure 12. Comparison of inductance values between two machines

The power factor and inductance are shown in Fiugre 11 and Figure 12. As illustrated in Figure 10, inserting PMs drastically improves the power factor from 0.66 in the pure SynRM to 0.82 in the PMa-SynRM, achieving a 24% enhancement. This improvement is fundamentally tied to the inductance variations shown in Figure 12. While the q-axis inductance (L_q) for both machines remains nearly identical at approximately 0.58 H, the d-axis inductance (L_d) of the PMa-SynRM is significantly reduced to 0.0922H (compared to 0.1918H in the pure SynRM). This reduction is driven by the opposing magnetic field produced by the PMs along the d-axis.

4. CONCLUSION

This study successfully demonstrates that the PMa-SynRM effectively overcomes the two primary limitations of conventional SynRM: relatively low torque capability and a low power factor. Detailed comparative analysis confirms that inserting PMs into the rotor's flux barriers yields a 28% increase in electromagnetic torque and a 24% improvement in the power factor. In addition to quantifying these performance gains, this research thoroughly discusses critical design considerations, emphasizing the necessity of balancing magnet strength, iron rib thickness, and air-gap dimensions to prevent deep core saturation while ensuring mechanical integrity.

Ultimately, these findings establish a robust theoretical foundation for domestic researchers and engineers. The provided guidelines will facilitate the efficient development of advanced synchronous motors that offer versatile controllability, superior cooling, and higher fault tolerance than equivalent induction motors, all while maintaining lower manufacturing costs compared to traditional permanent magnet machines.

ACKNOWLEDGMENT

This research is funded by Hanoi University of Industry under project number 10-2024-RD/HD-DHCN.

REFERENCES

[1]. X. Li, Y. Wang, Y. Cheng, D. Li, R. Qu, "An Overview of High-efficiency Synchronous Reluctance Machines," *CES Trans. Electr. Mach. Syst.*, 7, 1, 81-91, 2023. doi: 10.30941/CESTEMS.2023.00030.

[2]. R. Vartanian, H. A. Toliyat, "Design and comparison of an optimized permanent magnet-assisted synchronous reluctance motor (PMa-SynRM) with an induction motor with identical NEMA frame stators," in *IEEE Electric Ship Technologies Symposium, ESTS 2009*, IEEE, 107-112, 2009. doi: 10.1109/ESTS.2009.4906501.

[3]. M. Ferrari, N. Bianchi, E. Fornasiero, "Analysis of rotor saturation in synchronous reluctance and PM-assisted reluctance motors," *IEEE Trans. Ind. Appl.*, 51, 1, 169-177, 2015. doi: 10.1109/TIA.2014.2326056.

[4]. D. G. Dorrell, "The challenges of meeting IE4 efficiency standards for induction and other machines," in *Proceedings of the IEEE International Conference on Industrial Technology*, IEEE, 213-218, 2014. doi: 10.1109/ICIT.2014.6894941.

[5]. M. Murataliyev, *Novel sizing and modeling techniques for synchronous reluctance machines*, University of Nottingham (United Kingdom), 2021. [Online]. Available: http://eprints.nottingham.ac.uk/64494/

[6]. G. Gallicchio, M. Palmieri, F. Cupertino, M. Di Nardo, M. Degano, C. Gerada, "Permanent Magnets Assistance Design Methods of High-Speed Synchronous Reluctance Machines," in *2022 IEEE Energy Conversion Congress and Exposition, ECCE 2022*, IEEE, 1-8, 2022. doi: 10.1109/ECCE50734.2022.9947998.

[7]. J. H. Lee, Y. J. Jang, J. P. Hong, "Characteristic analysis of permanent magnet-assisted synchronous reluctance motor for high power application," *J. Appl. Phys.*, 97, 10, 10Q503, 2005. doi: 10.1063/1.1851831.

[8]. Thanh Anh Huynh, Min-Fu Hsieh, Kai-Jung Shih, Hsiu-Fu Kuo, "Design and analysis of permanent-magnet assisted synchronous reluctance motor," in *2017 20th International Conference on Electrical Machines and Systems (ICEMS)*, IEEE, 2017. doi: https://doi.org/10.1109/ICEMS.2017.8056462.

[9]. A. Gunnarson, L. Johansson, *Synchronous Reluctance Motor and Drive System Design for Handheld Applications*. Master's thesis in Electric Power Engineering, Chalmers University of Technology, Gothenburg, 2022.

[10]. G. Pellegrino, T. M. Jahns, N. Bianchi, W. Soong, F. Cupertino, "The Rediscovery of Synchronous Reluctance and Ferrite Permanent Magnet Motors," *Rediscovery Synchronous Reluctance Ferrite Perm. Magn. Mot. - Tutor. Course Notes*, 1–136, 2016. [Online]. Available: http://link.springer.com/10.1007/978-3-319-32202-5

[11]. R. R. Moghaddam, F. Magnussen, C. Sadarangani, "Synchronous Reluctance Machine (SynRM) Design," *Kth*, 1-103, 2007. [Online]. Available: http://www.diva-portal.org/smash/get/diva2:753114/FULLTEXT01.pdf